Journal of Experimental Botany, Vol. 58, No. 8, pp. 2181–2191, 2007
doi:10.1093/jxb/erm092 Advance Access publication 22 May, 2007
This paper is available online free of all access charges (see http://jxb.oxfordjournals.org/open_access.html for further details)

Journal of Experimental Botany
www.jxb.oxfordjournals.org

RESEARCH PAPER

Mutational evidence that the *Arabidopsis* MAP kinase MPK6 is involved in anther, inflorescence, and embryo development

Susan M. Bush and Patrick J. Krysan*

Genome Center of Wisconsin and Department of Horticulture, 1575 Linden Drive, University of Wisconsin, Madison, WI 53706, USA

Received 20 February 2007; Revised 29 March 2007; Accepted 4 April 2007

Abstract

Loss-of-function, dominant-negative, and change-of-function genetic approaches were used to investigate the role played by the *Arabidopsis* mitogen-activated protein (MAP) kinase MPK6 throughout development. Plants homozygous for T-DNA null alleles of *MPK6* displayed reduced male fertility and abnormal anther development. In addition, a portion of the seed produced by *mpk6* plants was found to contain embryos that had burst out of their seed coats. To address potential functional redundancy, a dominant-negative version of *MPK6* was constructed by changing the TEY activation loop motif to the amino acid sequence AEF. Plants expressing *MPK6AEF* via the *MPK6* native promoter were found to produce excessive stomata, consistent with the recently described role of MPK6 in stomatal patterning. A novel floral phenotype characterized by abnormal sepal development was also observed in *MPK6AEF* lines. The gene expression pattern of the *MPK6* native promoter was determined using a *YFP–MPK6* fusion construct, and expression was observed throughout most plant tissues, consistent with a role for MPK6 in multiple developmental processes. The *YFP–MPK6* construct was found to rescue the fertility phenotype of *mpk6* null alleles, indicating that the fusion protein retains its biological activity. It was also observed, however, that plants expressing *YFP–MPK6* displayed reduced apical dominance and a shortening of inflorescence internodes. These results suggest that the YFP tag modifies the activity of MPK6 in a manner that affects inflorescence development but not anther development. Taken together, the present results indicate that MPK6 is involved in the regulation of multiple aspects of plant development.

Key words: Anther development, *Arabidopsis*, embryo development, floral development, MAP kinase, MPK6.

Introduction

Mitogen-activated protein (MAP) kinase cascades are conserved signalling pathways that regulate diverse aspects of growth, development, and stress response in all eukaryotes. The genome of *Arabidopsis* encodes 20 MAP kinase isoforms (MAPK-Group, 2002), and much experimental effort has been devoted to determining the biological processes that are regulated by each of these kinases. The particular MAP kinase isoforms MPK3, MPK4, and MPK6 have been the most extensively studied to date. Both biochemical and genetic analyses have been reported for each of these isoforms, and the emerging picture of MPK3, MPK4, and MPK6 signalling is one of complexity (Mishra *et al*., 2006). Each of these proteins appears to serve in multiple signalling pathways, and at our current level of understanding there seems to be significant functional redundancy between these three proteins. For example, it has been observed that plants exposed to hydrogen peroxide or pathogen-associated molecular patterns (PAMPs) respond by rapidly activating the kinase activities of MPK3, MPK4, and MPK6 (Ichimura *et al*., 2006; Nakagami *et al*., 2006; Suarez-Rodriguez *et al*., 2007). The activation of MPK4 by these signals is dependent on the upstream MAP kinase kinase kinase (MAP3K) MEKK1, whereas activation of MPK3 and MPK6 is not (Ichimura *et al*., 2006; Nakagami *et al*.,

* To whom correspondence should be addressed. E-mail: fpat@biotech.wisc.edu

2006; Suarez-Rodriguez *et al*., 2007). These results indicate that a given stimulus can activate all three MAP kinases, but via at least two distinct pathways. Genotoxic stress, in contrast, has been shown to activate only MPK6 (Ulm *et al*., 2002), while ozone treatment activates both MPK3 and MPK6 (Miles *et al*., 2005). Upstream of the MAP kinases, the MAP kinase kinase (MAP2K) protein MKK1 has been shown to activate MPK4 after PAMP treatment (Meszaros *et al*., 2006), and after cold and salt stress MKK2 activates MPK4 and MPK6 (Teige *et al*., 2004). MKK4 and MKK5 activate the kinase activities of MPK3 and MPK6 after PAMP exposure (Asai *et al*., 2002) and in the stomatal patterning pathway (Wang *et al*., 2007). These biochemical studies have indicated that a variety of stress treatments result in the activation of different combinations of the three MAP kinase isoforms MPK3, MPK4, and MPK6.

In addition to these biochemical studies, genetic analyses have also been performed for MPK3, MPK4, and MPK6 (Petersen *et al*., 2000; Menke *et al*., 2004; Miles *et al*., 2005; Wang *et al*., 2007). Null alleles of *mpk4* generated by transposon-based mutagenesis have been shown to cause a dwarf plant phenotype due to the constitutive activation of the systemic acquired resistance (SAR) pathway (Petersen *et al*., 2000; Brodersen *et al*., 2006). This analysis established *MPK4* as a negative regulator of salicylic acid-dependent defence response genes. A deletion null allele of *mpk3* isolated by reverse-genetic screening of fast neutron-mutagenized *Arabidopsis* has been described by Miles *et al*. (2005) and found to cause an ozone-hypersensitive phenotype. This same study used RNA interference (RNAi) to demonstrate that reduced levels of MPK6 also result in ozone hypersensitivity (Miles *et al*., 2005). This work indicated that MPK3 and MPK6 may play overlapping roles in oxidative stress response signalling. In a separate study, Menke *et al*. (2004) also used an RNAi approach to study *MPK6* function. These authors observed no abnormal developmental phenotypes in *MPK6* RNAi lines but did report compromised resistance to both virulent and avirulent pathogens (Menke *et al*., 2004). Unlike *mpk4* mutants, however, these *MPK6* RNAi lines did not affect regulation of the SAR response.

The most recent genetic analysis of *MPK3* and *MPK6* involved the use of T-DNA null alleles of both loci. In this study, Wang *et al*. (2007) reported that no obvious developmental phenotypes were apparent in the *mpk3* or *mpk6* single mutant lines. The double mutant state, however, was found to be embryo lethal. A conditional rescue strategy based on the dexamethasone-inducible promoter was therefore used to overcome the embryo-lethal phenotype and allow observation of the double mutant state later in development. These experiments demonstrated that *MPK3* and *MPK6* are required for the proper regulation of stomatal patterning in leaf tissue. The absence of MPK3/6 activity causes excessive stomata, while excessive MPK3/6 activity results in an absence of stomata. Additionally, silencing of the MAP2Ks *MKK4*/*5* using tandem RNAi resulted in a stomatal patterning defect similar to that of the *mpk3*/*mpk6* double mutant, demonstrating that MKK4/5 are upstream of MPK3/6 (Wang *et al*., 2007).

These published genetic experiments, in conjunction with the extensive biochemical investigations that have been reported, indicate that MPK3, MPK4, and MPK6 are involved in the regulation of both stress response and developmental pathways. In the present study a thorough genetic analysis of the *MPK6* locus was performed in order to determine if there are additional developmental pathways that make use of MPK6 that have not yet been described. Through the use of loss-of-function, dominant-negative, and change-of-function approaches, several additional aspects of *Arabidopsis* development that are influenced by MPK6 have been identified. This information serves to broaden our understanding of the many processes that fall under the influence of MAP kinase signalling in *Arabidopsis*.

Materials and methods

Plant growth conditions and mutants

Arabidopsis plants were grown on soil under constant light at 22 °C. Plants with T-DNA insertions within *MPK6* (At2g43790) were obtained from the Salk T-DNA collection (Alonso *et al*., 2003). SALK_073907 has previously been described as *mpk6-2* (Liu and Zhang, 2004); SALK_062471 is denoted here as *mpk6-4*. The *mpk3* mutant used for these studies (SALK_151594) has been described previously (Wang *et al*., 2007). PCR primers as follows were used for genotyping the plants: MPK6-F2, 5′-GCCTCAGATGCCTGGGATTGAGAATATTC-3′; MPK6-RT-R2, 5′-AGAGTGGCTTACGGTCCATTAACTCCATG-3′; p745, 5′-AACGTCCGCAATGTGTTATTAAGTTGTC-3′; MPK3-F, 5′-CCGAGCAATCTTCTGTTGAACGCGAATTG-3′; and MPK3-R, 5′-TGCTGCACTTCTAACCGTATGTTGGATTG-3′. p745 anneals to the T-DNA left border. Sequencing of the T-DNA flanking sequence for each allele confirmed the identity of the mutated gene and precisely mapped the insert location. All wild-type and mutant plants used in this work are in the Columbia-0 ecotype.

Reverse transcriptase-PCR analysis of gene expression levels

RNA was isolated from plant tissue using the RNeasy Plant Mini Kit (Qiagen, Valencia, CA, USA). cDNA was reverse-transcribed from DNase-treated total RNA using the SuperScript II First Strand cDNA Synthesis System (Invitrogen, Carlsbad, CA, USA). Quantitative real-time PCR analysis was carried out on an iCycler iQ™ real-time PCR detection system (Bio-Rad, Hercules, CA, USA) using the following gene-specific primers for *MPK6* and the histone gene *His2A* as a control: MPK6-RT-F2, 5′-GAGGACTCTCCGTGAGATCAAGCTGCTTC-3′; MPK6-RT-R2, 5′-AGAGTGGCTTACGGTCCATTAACTCCATG-3′; H2A-F2, 5′-CGATTTTTGAAAGCCGGTAAGTACGCCGA-3′; and H2A-R2, 5′-GCAACTTGCTTAGCTCCTCATCATTCCTC-3′.

Plasmid constructions

The wild-type *MPK6* genomic locus was amplified from wild-type Columbia-0 genomic DNA using the primers MPK6G-F1, 5′-AAAGAAGCTTGGAAAGCAAAGATAAATA-3′, and MPK6G-R2, 5′-AAGGAGAGAGAGCTCACAGATGAAAGT-3′, and cloned into a plasmid vector. These primers amplify a region containing ~2 kb of promoter sequence, the complete *MPK6* coding sequence, and ~1 kb of downstream sequence. DNA sequencing was used to confirm that the resulting *MPK6* genomic clone did not contain any PCR-induced mutations. For the genetic rescue experiments, this wild-type MPK6 genomic clone was moved into the T-DNA binary vector pCAMBIA3300S (Krysan *et al*., 2002) and introduced into plants via *Agrobacterium*-mediated transformation (Clough and Bent, 1998).

The *MPK6* amplicon described above was used to create the *YFP–MPK6* fusion. Unique *Aat*II and *Spe*I restriction sites were added directly 3′ of the *MPK6* start codon using site-directed mutagenesis. The yellow fluorescent protein (YFP)-coding sequence was then PCR amplified and cloned into the *MPK6* construct using sticky ends created by *Aat*II and *Nhe*I digestion. The resulting *N*-terminal *YFP–MPK6* fusion was moved into the T-DNA binary vector pCAMBIA3300S (Krysan *et al*., 2002) and introduced into wild-type Columbia-0, *mpk6-4*, and *mpk6-2* plants via *Agrobacterium*-mediated transformation (Clough and Bent, 1998).

The wild-type *MPK6* amplicon was also used to create the dominant-negative *MPK6AEF* construct. For this construct, the two codons specifying the activation loop residues of MPK6 were modified using site-directed mutagenesis to effect the following changes: T221A and Y223F (Bardwell *et al*., 1998). The resulting *MPK6AEF* construct was introduced into *Arabidopsis* plants as stated above.

Microscopic analysis

To monitor anther development, floral inflorescences of wild-type Columbia-0 and *mpk6-2* were fixed in Spurr's resin, dissected into 8–10 mm thin sections, and stained for visualization with 0.05% toluidine blue. Sections were viewed with bright-field illumination.

Environmental scanning electron microscopy (ESEM) was performed using a Quanta 200 ESEM. Fresh cotyledons from 3-d-old wild-type Columbia-0 and *mpk6-4+MPKAEF* plants grown on 0.5× Murashige and Skoog salt mixture medium with 1% agar (w/v) (MS medium) were placed in the microscope and scanned at 20 kV under 2–4 Torr pressure. The ESEM was also used to examine dehiscent anthers of wild-type and *mpk6-2* plants, and developing floral buds of wild-type and *MPK6AEF* plants.

Three-day-old seedlings expressing YFP–MPK6 were observed using confocal microscopy with a Zeiss Axiovert 100M inverted microscope with Bio-Rad MR1024 laser scanning. A 514 nm laser line from an argon ion laser was used to excite YFP, with the fluorescence emission collected by a broad band-pass filter (480–550 nm). Additionally, an Olympus BX60 compound microscope equipped for epifluorescence analysis of YFP fluorescence was used on cotyledon and floral tissue of plants expressing YFP–MPK6.

Results

mpk6 *null alleles cause reduced male fertility due to defects in anther development*

Two independent T-DNA null alleles of *mpk6* were obtained from the Salk T-DNA collection, and the precise T-DNA insertion sites were determined by DNA sequence analysis (Fig. 1A). The T-DNA insertion in *mpk6-2* lies within the fourth exon and that of *mpk6-4* is within the third exon. Both of these alleles constitute RNA null mutations based on reverse transcriptase-PCR (RT-PCR) analysis of homozygous individuals (Fig. 1A). Previous reports have indicated that no obvious developmental phenotypes are present in *mpk6* mutant plants (Menke *et al*., 2004; Wang *et al*., 2007). Under the growth conditions used for the present experiments, however, a significant reduction in the fertility of plants homozygous for either of the *mpk6* alleles was observed. In a wild-type *Arabidopsis* plant, silique elongation is dependent on successful fertilization and subsequent seed development. Silique length therefore constitutes a convenient measure of fertility. As shown in Fig. 1B and C, silique length in *mpk6* homozygous plants is ~50% less than that of the wild type. Although *mpk6* plants have a dramatic reduction in fertility, a small amount of seed is produced by these lines, allowing homozygous individuals to be propagated. Hand pollination of these partially fertile *mpk6* plants with wild-type pollen restored the *mpk6* siliques to a wild-type size, indicating that a defect in male fertility was responsible for the observed phenotype (data not shown).

The fact that reduced fertility was observed using two independent alleles of *mpk6* provided strong evidence that this phenotype was caused by mutation of the *MPK6* locus. In order to confirm this causal role, a genetic rescue experiment was performed by cloning a copy of the wild-type *MPK6* genomic locus, moving it into a T-DNA vector, and introducing this construct into *mpk6-2* and *mpk6-4* plants. This ectopic copy of the *MPK6* locus restored full fertility to both the *mpk6-2* and *mpk6-4* mutant plants, further confirming that mutation of the *MPK6* gene is responsible for the reduced male fertility phenotype (data not shown).

One additional aspect of the reduced fertility phenotype that warrants discussion is the fact that this phenotype displays variable penetrance. Under certain growth conditions, progeny from a homozygous *mpk6* plant will display a level of fertility that approaches that of the wild type. Under other conditions, however, progeny from that same plant will all display greatly reduced fertility. This variable penetrance may explain why previous studies of *mpk6* mutant lines did not report any notable developmental defects. An attempt was made to pinpoint the specific environmental variable that enhanced or suppressed the partial-fertility phenotype by testing different combinations of temperature, humidity, photoperiod, and light intensity. Despite these efforts, the specific environmental factor that tipped the balance between low and high fertility in *mpk6* mutant lines could not be determined. It should be noted, however, that even under the most favourable conditions the *mpk6* plants never achieve the full fertility of the wild type.

In order to characterize further the nature of the *mpk6* reduced male fertility phenotype, *mpk6* stigmas were hand

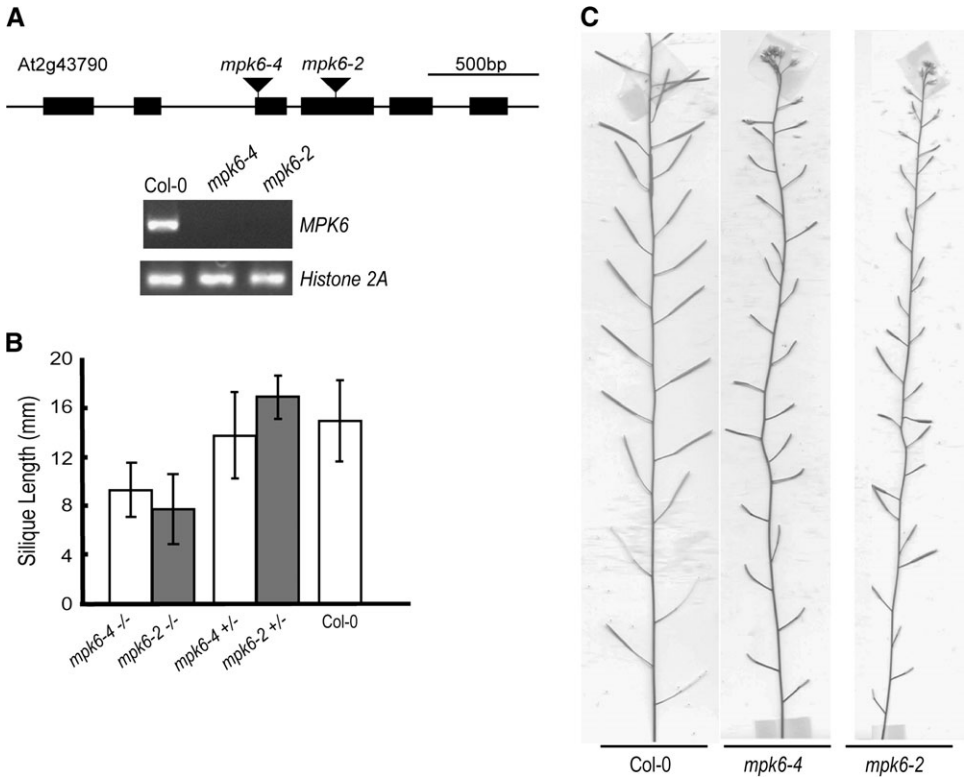

Fig. 1. Mutant alleles of *MPK6* display decreased fertility. (A) Genomic structure of the *Arabidopsis MPK6* locus. Exons are indicated by thick lines; T-DNA insertions are indicated by triangles. Lower panel: RT-PCR analysis of *MPK6* expression in wild-type Columbia-0 and homozygous *mpk6* mutant plants. The histone gene *His2A* was used as an internal control. (B) Mature silique length measurements of *mpk6* homozygous, *mpk6* heterozygous, and wild-type plants identified from segregating populations of *mpk6-4* and *mpk6-2* plants. Bars indicate standard deviation from the mean. (C) Wild-type and homozygous *mpk6* inflorescences demonstrating the reduced silique length of *mpk6* mutants.

pollinated using anthers from the same *mpk6* plant. This treatment rescued the reduced fertility phenotype, indicating that *mpk6* plants are able to produce at least some quantity of viable pollen grains (data not shown). *mpk6* plants therefore seem to be defective in the process of efficiently transferring pollen from anther to stigma. Microscopic analysis was next performed in order to search for possible structural defects that would explain the reduced male fertility. To begin, filament length of the anthers was measured since a common cause of reduced male fertility is a reduction in filament length preventing the anthers from reaching the stigma. No significant difference was observed in the lengths of wild-type, *mpk6-2*, and *mpk6-4* filaments (Fig. 2A; Table 1). ESEM was next used to study anther morphology and it was observed that *mpk6* anthers are substantially smaller in size than those of the wild type (Fig. 2B, C). In addition, the individual pollen grains on *mpk6* anthers appear to be more tightly associated with the anther when compared with wild type at the same developmental stage, and *mpk6* pollen grains may be larger than those of the wild type. Light microscopy of semi-thin sections confirmed that *mpk6* anthers were substantially smaller than those of the wild type (Fig. 2D, E). The structural defects observed in *mpk6* anthers may be responsible for compromising the efficiency of pollination in these plants, resulting in decreased male fertility.

mpk6 *null alleles cause a defect in embryo development*

As part of a comprehensive survey of the development of *mpk6* mutant plants, it was observed that a substantial portion of the seed collected from homozygous *mpk6-2* and *mpk6-4* plants displayed an unusual phenotype in which the embryo was found to be protruding out of the dried seed coat. In order to determine the point in seed development when this abnormality arose, siliques were dissected from plants at various stages and the seeds were observed using light microscopy. As shown in Fig. 3, protruding embryos were detected in *mpk6* siliques containing green seeds that had not begun the desiccation stage of seed development. Approximately 7% of the seed produced by *mpk6* plants display this protruding embryo phenotype (Table 2). An ectopic copy of the wild-type *MPK6* locus provides full rescue of the protruding embryo phenotype (Table 2).

A survey of the literature indicated that an identical phenotype has been reported for plants carrying a mutation

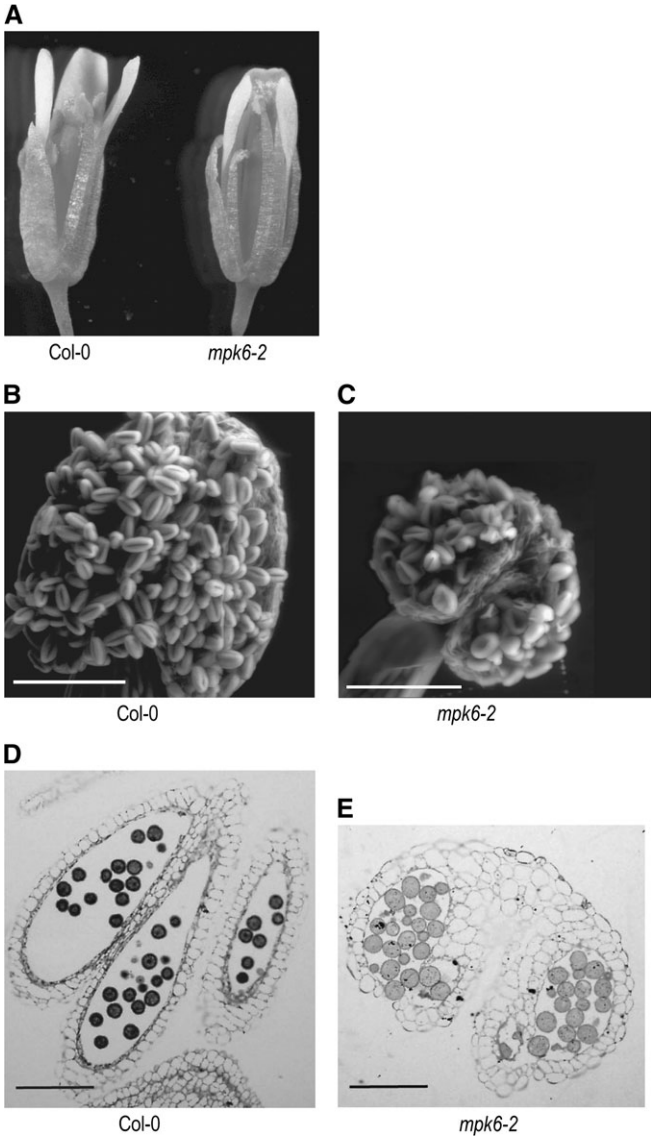

Fig. 2. Anther defects are present in *mpk6* plants. (A) The stamens of wild-type Columbia-0 and homozygous *mpk6-2* flowers are not different in length. (B, C) Environmental scanning electron microscope images of wild-type (B) and *mpk6-2* (C) anthers. Bars indicate 100 μm. (D, E) Thin sections through wild-type (D) and *mpk6-2* (E) anthers collected at the same developmental stage. Bars indicate 200 μm.

Table 1. *Stamen filament length*

Stamens were dissected from flowers with dehiscent anthers, and images were collected using light microscopy. Mean stamen length is reported together with the SD.

	Length (mm)	SD
Col-0	2.2	0.29
mpk6-2	2.2	0.23
mpk6-4	2.2	0.33

in the *YODA* gene (Lukowitz *et al*., 2004), which is a MAP3K that has recently been shown to act upstream of MPK6 and MPK3 to regulate stomatal patterning (Bergmann *et al*., 2004; Wang *et al*., 2007). In addition to its role in stomatal development, YODA has also been shown to be required for suspensor development during embryogenesis (Lukowitz *et al*., 2004). *yoda* loss-of-function mutants fail to develop a normal suspensor, thereby causing the embryo to become pinned between the walls of the developing seed coat. The resulting physical constraints often cause the embryo to pop out of the seed coat during the course of seed development. The observation of the protruding embryo phenotype in *mpk6* plants provides direct genetic evidence that MPK6 acts downstream of YODA in the regulation of embryonic development. Additionally, Wang *et al*. (2007) demonstrated that $mpk3^{-/-}$ $mpk6^{-/-}$ embryos improperly regulate asymmetric division of the zygote. As a result of these data, and because of the previously described genetic redundancy of MPK3 and MPK6 in the stomatal patterning pathway, seed produced by an *mpk3* plant were next analysed, but no protruding embryos were detected (Fig. 3D). The differential effects of *mpk3* and *mpk6* on embryo development suggest that genetic redundancy between these loci is not complete in the context of embryo development.

A dominant-negative form of MPK6 *causes defects in floral development*

Loss-of-function alleles represent one genetic strategy for elucidating gene function, but a drawback to this approach is that genetic redundancy can mask the appearance of instructive phenotypes in single mutant lines. In the case of *MPK6*, it has been previously demonstrated that there is significant redundancy between *MPK3* and *MPK6* (Wang *et al*., 2007). It was therefore of interest to determine if alternative genetic approaches would result in the identification of additional development roles for MPK6. Toward this end, a version of the *MPK6* gene that encoded a dominant-negative protein was constructed by mutating the coding region such that the canonical TEY activation loop motif was changed to AEF (Bardwell *et al*., 1998; Petersen *et al*., 2000). The resulting protein should not be able to be phosphorylated by any of its upstream MAP2K partner(s) such as MKK4/5 (Wang *et al*., 2007), and therefore should serve to block signalling in its cognate pathways. This *MPK6AEF* construct uses the *MPK6* native promoter to drive transcription.

The *MPK6AEF* construct was introduced into wild-type Columbia and *mpk6* mutant backgrounds, and several independent transgenic lines were isolated for each background. An overproduction of stomata was observed in the leaf epidermis of lines expressing *MPK6AEF* in either the wild-type or *mpk6* mutant backgrounds (Fig. 4D). This result indicated that MPK6AEF is able to overcome the redundancy of MPK3 and block signalling through the YODA–MPK3/6 pathway that regulates stomatal patterning

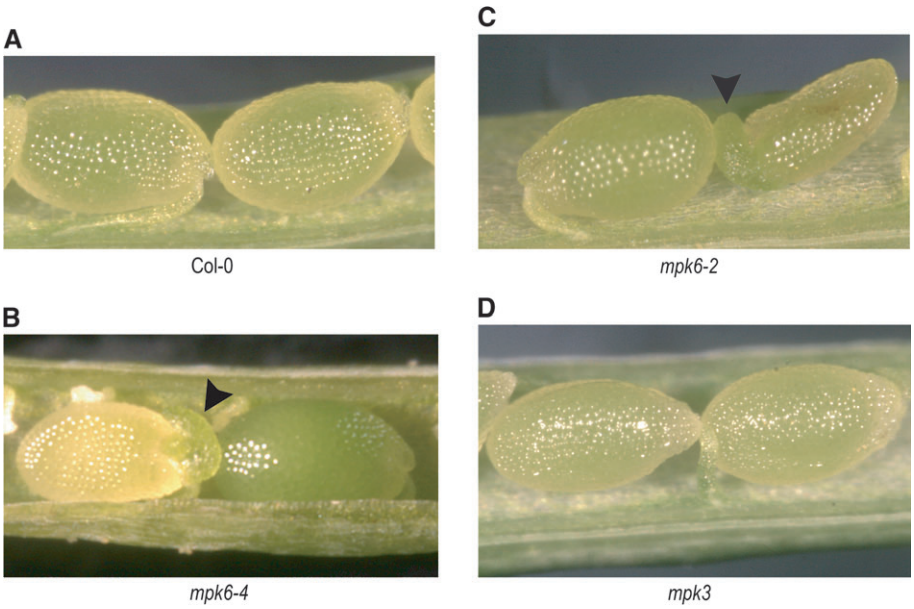

Fig. 3. *mpk6* embryos often burst out of their constraining seed coats. Developing green seeds in the siliques of wild-type Columbia-0 (A), *mpk6-4* (B), *mpk6-2* (C), and *mpk3* (D) plants. Only *mpk6* mutants display embryos that have burst out of their surrounding seed coat (arrowheads).

Table 2. *Frequency of seeds displaying exposed embryos*

Seeds from green siliques were observed using light microscopy, and the number of seeds which burst from their seeds coats was counted.

	Burst seeds	Total seeds	Percentage
Col-0	0	259	–
mpk6$^{-/-}$	62	851	7%
mpk6$^{-/-}$*+MPK6*	0	1156	–
mpk6$^{-/-}$*+YFP–MPK6*	0	621	–
Col-0+*MPK6AEF*	16	518	3%

(Bergmann *et al*., 2004; Wang *et al*., 2007). RT-PCR analysis was used to measure the expression level of *MPK6AEF* in three independent transgenic lines. Expression ranged from ~2- to ~6-fold that of wild-type *MPK6* (Fig. 4B). These modest levels of *MPK6AEF* expression should minimize the likelihood that the MPK6AEF protein interferes with signalling in pathways that are not normally regulated by wild-type MPK6.

In addition to the stomatal patterning phenotype, a novel floral development phenotype was also observed in MPK6AEF lines (Fig. 5A, B). The most striking aspect of this phenotype is that the sepals of developing flowers are substantially shorter than the carpels and bend outward at the tips. This situation causes the flowers to open at a very early stage in development (Fig. 5C, D). In addition, the overall length of the flowers produced by *MPK6AEF* plants is substantially shorter than that of the wild type. ESEM analysis indicated that reduced cell elongation in the carpel epidermis was at least partially responsible for this size reduction (Fig. 5E, F). The floral development phenotype was observed in seven independent transgenic lines expressing the *MPK6AEF* construct in both the wild-type and *mpk6* mutant backgrounds.

MPK6 *gene expression pattern*

It was observed that *MPK6* influences a diverse set of developmental processes. One would therefore predict that MPK6 would be expressed in a variety of tissues in *Arabidopsis*. In order to test this hypothesis directly, a *YFP–MPK6* fusion was constructed and placed under the transcriptional control of the *MPK6* native promoter. Transgenic lines were generated by transforming this construct into both wild-type and *mpk6* mutant backgrounds. Gene expression was then monitored using epifluorescence and confocal microscopy at various stages of development. As shown in Fig. 6, a strong YFP–MPK6 signal was observed in floral tissues (Fig. 6A, B), leaves (Fig. 6C, D), hypocotyls (Fig. 6E), and roots (Fig. 6F). This broad expression pattern is consistent with MPK6 playing a role in multiple aspects of development.

The YFP–MPK6 fusion protein causes a novel inflorescence phenotype

When the YFP–MPK6 construct described above was transformed into *mpk6* mutant plants it was observed that the partial fertility and protruding embryo phenotypes were both rescued by this fusion protein (Table 2 and data not shown). These results indicated that the YFP tag did not interfere with the biological activity of MPK6. In

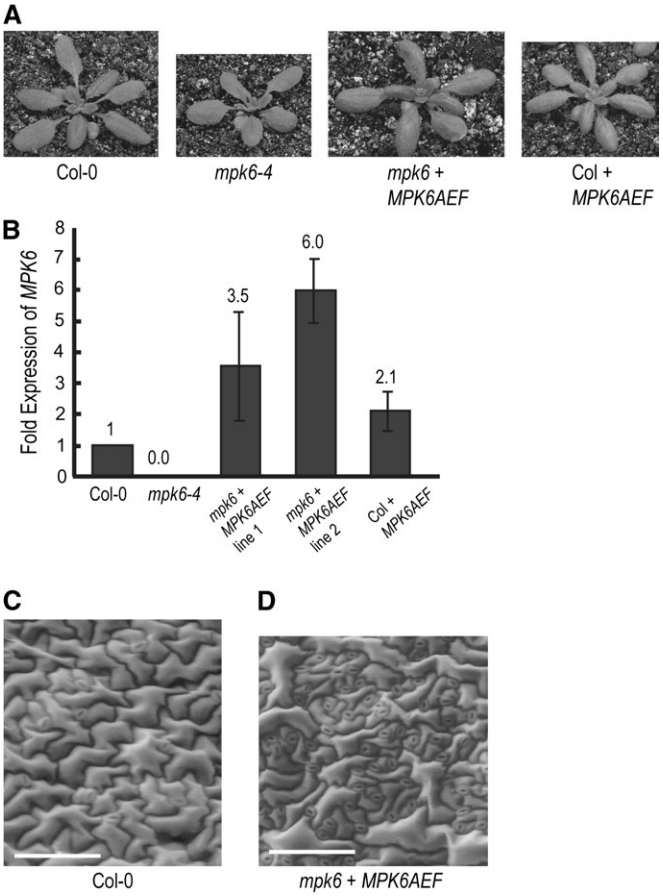

Fig. 4. Expression of the dominant-negative *MPK6AEF* causes stomatal patterning defects. (A) Three-week-old plants grown in soil. (B) Quantitative RT-PCR analysis of *MPK6AEF* expression. The expression level is normalized to that of *MPK6* in non-transgenic, wild-type Columbia. For the transgenic lines generated in the wild-type background, the reported expression level represents the sum of both endogenous *MPK6* and the transgenic *MPK6AEF* messages. The expression level for two independent *mpk6+MPK6AEF* lines is shown. (C, D) Environmental scanning electron microscope images of cotyledons of wild-type Columbia-0 (C) and *mpk6-4+MPK6AEF* (D) plants. Bars indicate 100 μm. *mpk6+MPK6AEF*, *mpk6-4* stably transformed with the dominant-negative *MPK6AEF* construct. Col+*MPK6AEF*, Columbia-0 stably transformed with the dominant-negative *MPK6AEF* construct.

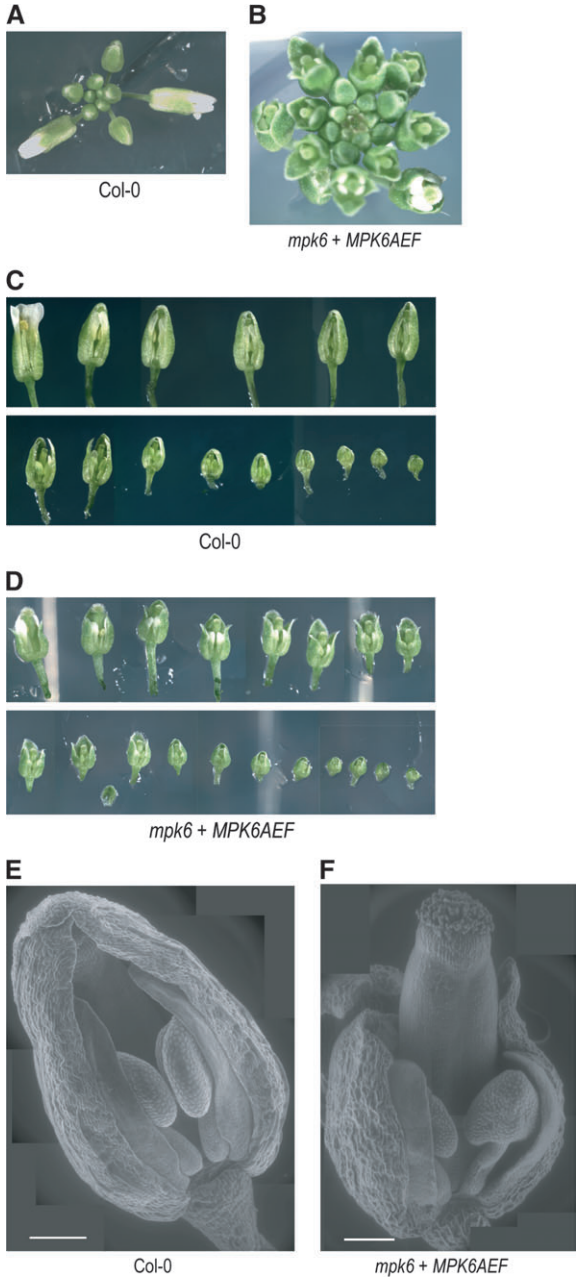

Fig. 5. Floral phenotype caused by the dominant-negative *MPK6AEF* construct. (A, B) Inflorescences of wild-type Columbia-0 (A) and *mpk6-4+MPK6AEF* (B). (C, D) Developmental series of floral buds in the wild type (C) and *mpk6-4+MPK6AEF* (D). (E, F) Environmental scanning electron microscope images of floral buds from the wild type (E) and *mpk6-4+MPK6AEF* (F) collected at the same developmental stage. Bars indicate 200 μm. *mpk6+MPK6AEF*, *mpk6-4* stably transformed with the dominant-negative *MPK6AEF* construct.

addition, however, a novel inflorescence phenotype was observed in several independent lines expressing *YFP–MPK6* in either the wild-type or *mpk6* mutant backgrounds. RT-PCR analysis indicated that these lines expressed *YFP–MPK6* at levels ranging from 1–5-fold that of wild-type *MPK6* (Fig. 7B).

The characteristic feature of the *YFP–MPK6* inflorescence phenotype is a decrease in apical dominance, accompanied in some cases by a shortening of the internodes between mature flowers (Fig. 7A). In the most drastic examples of this phenotype, the total height of the inflorescence of a mature *YFP–MPK6* plant does not exceed 3 cm. For comparison, wild-type plants typically exceed 30 cm in height at maturity. Despite this severe reduction in inflorescence height, the siliques produced by *YFP–MPK6* plants are fully fertile and elongate to the size of the wild type. This characteristic indicates that the plants do not suffer from a general reduction in

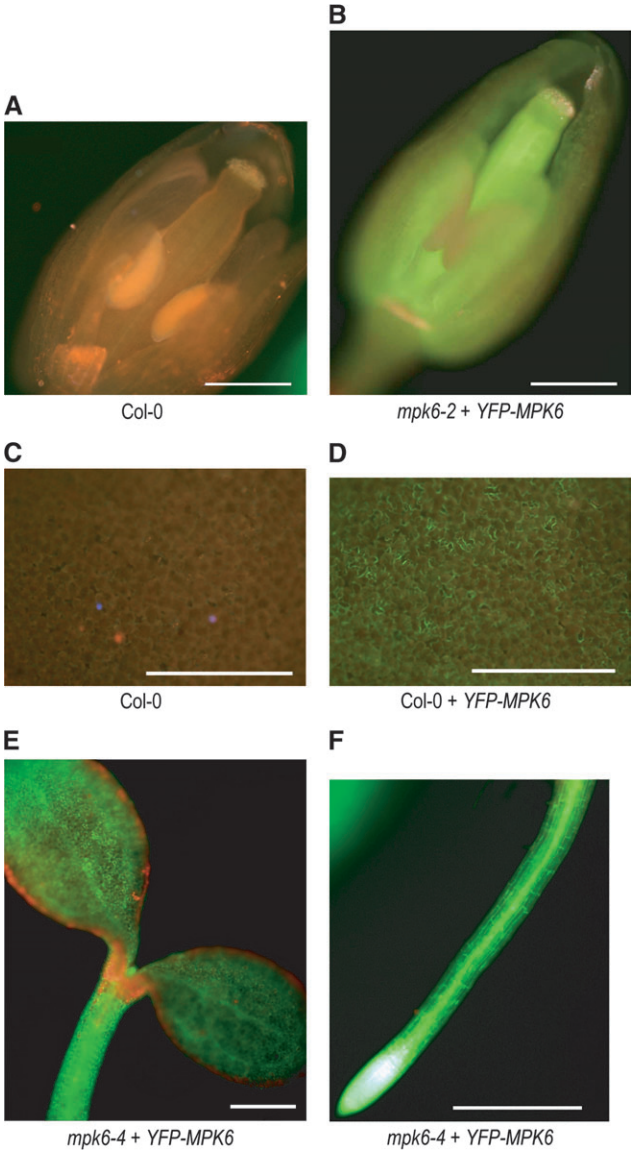

Fig. 6. *MPK6* displays a widespread pattern of gene expression. YFP–MPK6 expressed via the *MPK6* native promoter was observed with epifluorescence and confocal microscopy using *mpk6-4+YFP–MPK6* transgenic lines. (A, B) Floral buds of untransformed wild-type (A) and *mpk6-4+YFP–MPK6* (B) plants. Bars indicate 100 μm. (C and D) Rosette leaves of untransformed wild-type (C) and *mpk6-4+YFP–MPK6* (D) plants. Bars indicate 100 μm. Fluorescent signal in the YFP colour range is not observed in the wild-type Columbia-0 negative controls. (E, F) Confocal images of YFP–MPK6 fluorescence in cotyledons (E) and root tips (E) of a *mpk6-4+YFP–MPK6* seedling. Bars indicate 500 μm.

inflorescence growth, but rather have a defect that is specific to internode and stem elongation.

Discussion

Using a combination of genetic approaches, several developmental processes have been identified that appear to be influenced by the *Arabidopsis* MAP kinase MPK6. Previous reports on the genetic analysis of *MPK6* in *Arabidopsis* have indicated a role for this protein in disease resistance, ozone sensitivity, and stomatal patterning (Menke *et al*., 2004; Miles *et al*., 2005; Wang *et al*., 2007). None of these previous studies reported any reduction in fertility associated with mutation or suppression of *MPK6*, however, which is contrary to what was observed for the two independent T-DNA null alleles. Since two of these previous studies involved the use of RNAi to reduce the level of *MPK6* expression, it is possible that residual levels of MPK6 could explain this discrepancy because the RNAi approach does not always lead to complete gene silencing. It has also been reported, however, that no obvious developmental phenotypes were observed with one of the same T-DNA null alleles of *MPK6* that was characterized in the present study (Wang *et al*., 2007). The likely explanation for this discrepancy is variable penetrance of the male-sterile phenotype caused by *mpk6*, as discussed in the Results.

It was observed that the partial fertility of *mpk6* plants could be overcome by hand pollination using anthers from the same *mpk6* plant. This result suggested that *mpk6* plants were defective in the movement of pollen from anther to stigma. Microscopic analysis of *mpk6* anthers indicated that there was no change in filament length compared with the wild type, but that anther size was significantly reduced in the mutants. The structural abnormalities that were observed in *mpk6* anthers may prevent the efficient release of pollen, thereby resulting in partial male sterility.

The other novel phenotype that was observed in *mpk6* null mutants was a propensity for the embryos formed on these plants to burst out of their seed coat during the course of seed development. This phenotype was observed in both independent null alleles of *mpk6* and was rescued when an ectopic copy of wild-type *MPK6* was introduced into the null mutant background. This phenotype is identical to what has been described for plants carrying the *yoda* mutation (Lukowitz *et al*., 2004). *YODA* is a MAP3K that has been shown to regulate cell division in the suspensor during embryo development. *YODA* loss-of-function mutants have a shortened suspensor that can cause the developing embryo to be squeezed out of the seed coat during the course of seed development (Lukowitz *et al*., 2004). In addition to its role in suspensor formation, YODA has also been shown to act upstream of MPK3 and MPK6 to control stomatal patterning (Bergmann *et al*., 2004; Wang *et al*., 2007). The observation of a *yoda*-like embryonic phenotype in the *mpk6* mutant lines suggests that MPK6 acts downstream of YODA in the regulation of embryo development as well as stomatal patterning.

Because of the functional redundancy that has been documented for MPK3 and MPK6 (Wang *et al*., 2007), it was of interest to test additional genetic strategies for

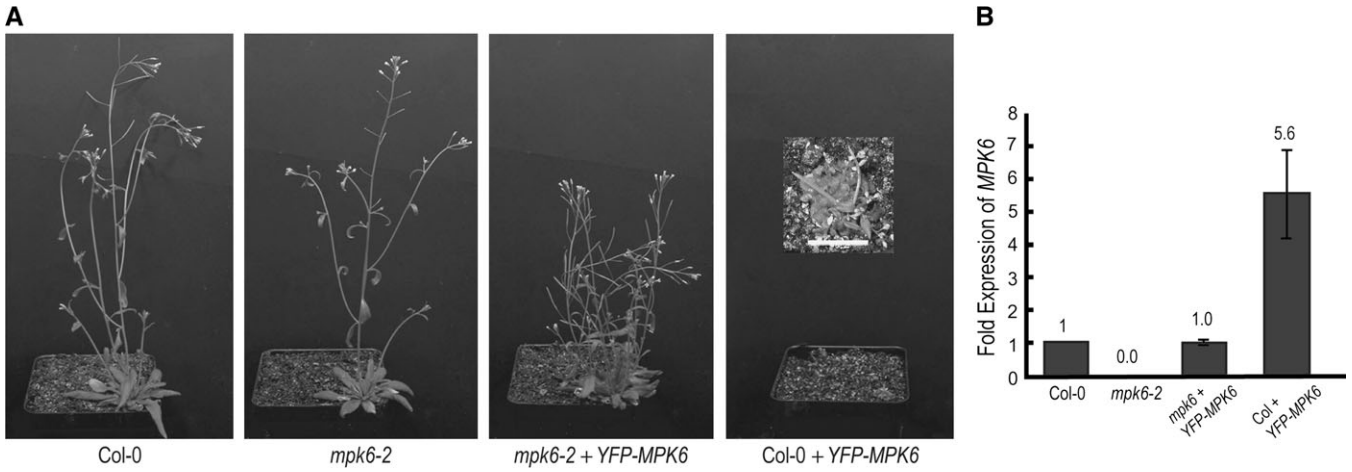

Fig. 7. *YFP–MPK6* expression causes a novel inflorescence phenotype. (A) Five-week-old plants grown in soil. Inset: Col+*YFP–MPK6* plant with severely shortened inflorescence internodes. Bar indicates 1 cm. The *mpk6-2*+*YFP–MPK6* plant displays an intermediate phenotype with a moderate loss of apical dominance. (B) Quantitative RT-PCR analysis of *YFP–MPK6* expression. The expression level is normalized to that of *MPK6* in non-transgenic, wild-type Columbia. For the transgenic lines generated in the wild-type background, the reported expression level represents the sum of both endogenous *MPK6* and the transgenic *YFP–MPK6* messages. Col+*YFP–MPK6*, Columbia-0 stably transformed with *YFP–MPK6*. *mpk6*+*YFP–MPK6*, *mpk6-2* stably transformed with *YFP–MPK6*.

investigating the function of MPK6. A mutant version of *MPK6* was therefore constructed in which the coding sequence for the kinase activation loop is mutated from the native TEY-coding sequence to one encoding AEF. The activation loop of a MAP kinase is a highly conserved motif that is specifically recognized by a cognate MAP kinase kinase (MAP2K) and doubly phosphorylated on the threonine and tyrosine residues (Bardwell *et al*., 1998). When these threonine and tyrosine residues are replaced with non-phosphorylatable alanine and phenylalanine residues, the resulting kinase should not be able to be activated by MAP2K phosphorylation. The premise for constructing this type of dominant-negative MAP kinase is that the mutant protein should have the capacity to assemble into the native signalling modules normally occupied by wild-type MPK6. Since this mutant form cannot be activated by the upstream MAP2K, however, signalling through this cascade should be blocked. If the MPK6AEF protein is expressed in the *mpk6* null mutant background, one would predict that the mutant protein may be able to serve as an effective physical barrier preventing other related MAP kinase isoforms from occupying the void created by the absence of wild-type MPK6 protein. In this way, the MPK6AEF protein could provide a tool for addressing genetic redundancy because it would prevent proteins such as MPK3 from taking over the signalling pathways left vacant in *mpk6* null mutants.

One potential drawback to the dominant-negative approach is that the MPK6AEF protein may have the capacity to interfere with MAP kinase cascades that do not normally make use of wild-type MPK6 protein. An attempt was made to minimize this potential complication by putting the *MPK6AEF* construct under the transcriptional control of the *MPK6* native promoter so that the resulting MPK6AEF protein would be present in similar cells and organs, and at levels similar to those of MPK6 in a wild-type plant. When this *MPK6AEF* construct was transformed into either wild-type or *mpk6* backgrounds, a pronounced increase in the number of stomata present in the leaf epidermis was observed, consistent with the *mpk3*/*mpk6* double mutant phenotype described by Wang *et al*. (2007). The ability of the *MPK6AEF* construct to interfere with the YODA–MKK4/5–MPK3/6 stomatal development pathway indicates that this dominant-negative approach provides an effective method for overcoming functional redundancy between MPK3 and MPK6.

In addition to the stomatal patterning phenotype which had previously been described by others, a novel floral phenotype was also observed in plants expressing the *MPK6AEF* construct. The characteristic features of this phenotype were a reduction in sepal and petal size and a pronounced bending of the sepals, resulting in flowers in which the carpel protrudes from the end of the flower very early in development. This novel phenotype indicates that MPK6 plays an important role in signalling pathways that dramatically affect floral organ development. In addition, it is apparent that functional redundancy is masking the appearance of this floral phenotype in *mpk6* null mutants, further demonstrating the value of using both dominant-negative and loss-of-function approaches to study gene function.

It has been observed both in the present study and by others that MPK6 is involved in embryo development, leaf development, and floral development (Wang *et al*., 2007). Correspondingly, expression of a *YFP–MPK6*

fusion, placed under the transcriptional control of the *MPK6* native promoter, indicated that *MPK6* is indeed expressed at detectable levels in most tissues of the plant, consistent with its observed functions throughout development. It was also demonstrated that the YFP–MPK6 fusion protein retains its biological activity, as it was able to rescue both the protruding embryo and reduced fertility phenotypes of *mpk6* null mutants.

The *YFP–MPK6* construct was also found to cause the appearance of a novel inflorescence phenotype characterized by reduced apical dominance and shortened internodes. This phenotype occurred in multiple, independent lines in both the wild-type Columbia and *mpk6* mutant backgrounds. In the case of *mpk6* plants expressing YFP–MPK6, the decrease in apical dominance was always accompanied by a complete rescue of the reduced fertility phenotype, indicating that the YFP–MPK6 protein is still active in these lines. Based on these results, it appears that the YFP tag is modifying the MPK6 protein in a way that differentially affects its ability to act in particular signalling pathways. It is possible that the signalling pathway affecting internode elongation is composed of different components from those of the pathway that affects anther development, and that the YFP tag interferes with the ability of MPK6 to interact with the internode-specific pathway but not the anther-specific pathway. More detailed structure–function studies using a variety of modified MPK6 fusion proteins could help explain why YFP–MPK6 rescues one *mpk6* mutant phenotype while at the same time generating a new mutant phenotype. No matter what the mechanistic explanation is for this novel situation, it serves to highlight the complexity inherent in MAP kinase signalling pathways in *Arabidopsis*.

It has been demonstrated that the use of a variety of genetic approaches can be an effective strategy for uncovering developmental pathways that utilize a specific MAP kinase in *Arabidopsis*. The three methods that were employed here (loss-of-function, dominant-negative, and change-of-function) each resulted in the identification of a different aspect of development that was affected by MPK6. MAP kinase signalling pathways may be particularly suited to this type of multifaceted approach because of the extensive complexity and redundancy that exists between these signalling molecules. Continued application of this type of approach to the many members of the MAP kinase gene family should help to improve our understanding of how plants manage and exploit the complexity inherent in MAP kinase signalling pathways.

Acknowledgements

The authors thank Shuqun Zhang for providing seed from the homozygous *mpk3* mutant line. This work was supported by a grant from the National Science Foundation (grant number MCB-0447750).

References

Alonso JM, Stepanova AN, Leisse TJ, *et al*. 2003. Genome-wide insertional mutagenesis of *Arabidopsis thaliana*. *Science* **301,** 653–657.

Asai T, Tena G, Plotnikova J, Willmann MR, Chiu WL, Gomez-Gomez L, Boller T, Ausubel FM, Sheen J. 2002. MAP kinase signalling cascade in Arabidopsis innate immunity. *Nature* **415,** 977–983.

Bardwell L, Cook JG, Voora D, Baggott DM, Martinez AR, Thorner J. 1998. Repression of yeast Ste12 transcription factor by direct binding of unphosphorylated Kss1 MAPK and its regulation by the Ste7 MEK. *Genes and Development* **12,** 2887–2898.

Bergmann DC, Lukowitz W, Somerville CR. 2004. Stomatal development and pattern controlled by a MAPKK kinase. *Science* **304,** 1494–1497.

Brodersen P, Petersen M, Bjorn Nielsen H, Zhu S, Newman MA, Shokat KM, Rietz S, Parker J, Mundy J. 2006. Arabidopsis MAP kinase 4 regulates salicylic acid- and jasmonic acid/ethylene-dependent responses via EDS1 and PAD4. *The Plant Journal* **47,** 532–546.

Clough SJ, Bent AF. 1998. Floral dip: a simplified method for *Agrobacterium*-mediated transformation of *Arabidopsis thaliana*. *The Plant Journal* **16,** 735–743.

Ichimura K, Casais C, Peck SC, Shinozaki K, Shirasu K. 2006. MEKK1 is required for MPK4 activation and regulates tissue-specific and temperature-dependent cell death in Arabidopsis. *Journal of Biological Chemistry* **281,** 36969–36976.

Krysan PJ, Jester PJ, Gottwald JR, Sussman MR. 2002. An Arabidopsis mitogen-activated protein kinase kinase kinase gene family encodes essential positive regulators of cytokinesis. *The Plant Cell* **14,** 1109–1120.

Liu Y, Zhang S. 2004. Phosphorylation of 1-aminocyclopropane-1-carboxylic acid synthase by MPK6, a stress-responsive mitogen-activated protein kinase, induces ethylene biosynthesis in Arabidopsis. *The Plant Cell* **16,** 3386–3399.

Lukowitz W, Roeder A, Parmenter D, Somerville C. 2004. A MAPKK kinase gene regulates extra-embryonic cell fate in Arabidopsis. *Cell* **116,** 109–119.

MAPK-Group. 2002. Mitogen-activated protein kinase cascades in plants: a new nomenclature. *Trends in Plant Sciences* **7,** 301–308.

Menke FL, van Pelt JA, Pieterse CM, Klessig DF. 2004. Silencing of the mitogen-activated protein kinase MPK6 compromises disease resistance in Arabidopsis. *The Plant Cell* **16,** 897–907.

Meszaros T, Helfer A, Hatzimasoura E, *et al*. 2006. The Arabidopsis MAP kinase kinase MKK1 participates in defence responses to the bacterial elicitor flagellin. *The Plant Journal* **48,** 485–498.

Miles GP, Samuel MA, Zhang Y, Ellis BE. 2005. RNA interference-based (RNAi) suppression of AtMPK6, an Arabidopsis mitogen-activated protein kinase, results in hypersensitivity to ozone and misregulation of AtMPK3. *Environmental Pollution* **138,** 230–237.

Mishra NS, Tuteja R, Tuteja N. 2006. Signaling through MAP kinase networks in plants. *Archives of Biochemistry and Biophysics* **452,** 55–68.

Nakagami H, Soukupova H, Schikora A, Zarsky V, Hirt H. 2006. A mitogen-activated protein kinase kinase kinase mediates reactive oxygen species homeostasis in Arabidopsis. *Journal of Biological Chemistry* **281,** 38697–38704.

Petersen M, Brodersen P, Naested H, *et al*. 2000. Arabidopsis map kinase 4 negatively regulates systemic acquired resistance. *Cell* **103,** 1111–1120.

Suarez-Rodriguez MC, Adams-Phillips L, Liu Y, Wang H, Su SH, Jester PJ, Zhang S, Bent AF, Krysan PJ. 2007. MEKK1 is required for flg22-induced MPK4 activation in Arabidopsis plants. *Plant Physiology* **143,** 661–669.

Teige M, Scheikl E, Eulgem T, Doczi R, Ichimura K, Shinozaki K, Dangl JL, Hirt H. 2004. The MKK2 pathway mediates cold and salt stress signaling in Arabidopsis. *Molecular Cell* **15,** 141–152.

Ulm R, Ichimura K, Mizoguchi T, Peck SC, Zhu T, Wang X, Shinozaki K, Paszkowski J. 2002. Distinct regulation of salinity and genotoxic stress responses by Arabidopsis MAP kinase phosphatase 1. *EMBO Journal* **21,** 6483–6493.

Wang H, Ngwenyama N, Liu Y, Walker JC, Zhang S. 2007. Stomatal development and patterning are regulated by environmentally responsive mitogen-activated protein kinases in Arabidopsis. *The Plant Cell* **19,** 63–73.